Growth and structural properties of m-plane ZnO on MgO (001) by molecular beam epitaxy

E. Cagin, J. Yang, W. Wang, J. D. Phillips, S. K. Hong et al.

Citation: Appl. Phys. Lett. **92**, 233505 (2008); doi: 10.1063/1.2940305
View online: http://dx.doi.org/10.1063/1.2940305
View Table of Contents: http://apl.aip.org/resource/1/APPLAB/v92/i23
Published by the American Institute of Physics.

Growth and structural properties of *m*-plane ZnO on MgO (001) by molecular beam epitaxy

E. Cagin,[1,a)] J. Yang,[1] W. Wang,[1] J. D. Phillips,[1] S. K. Hong,[2] J. W. Lee,[3] and J. Y. Lee[3]
[1]*Department of Electrical Engineering and Computer Science, The University of Michigan, Ann Arbor, Michigan 48109-2122, USA*
[2]*School of Nano Science and Technology, Chungnam National University, Daejeon 305-764, Republic of Korea*
[3]*Department of Materials Science and Engineering, Korea Advanced Institute of Science and Technology, Daejeon 305-701, Republic of Korea*

(Received 21 January 2008; accepted 19 May 2008; published online 10 June 2008)

The growth of wurtzite ZnO on cubic MgO (001) substrates by molecular beam epitaxy is reported. ZnO epilayers exhibit the nonpolar *m*-plane orientation based on x-ray diffraction and transmission electron microscopy analysis. Comparative studies of ZnO grown by pulsed laser deposition on MgO (001) result in preferred growth in the polar *c*-plane orientation. Investigation by high resolution transmission electron microscopy confirms an abrupt ZnO/MgO interface and monolayer spacing consistent with *m*-plane growth of ZnO. X-ray diffraction pole figures indicate two preferred rotational domains in-plane with a twist angle of 30°. © *2008 American Institute of Physics*. [DOI: 10.1063/1.2940305]

ZnO and its alloys make up an important system of II-VI compound semiconductors for novel electronic and optoelectronic devices. Alloys of ZnO with MgO and CdO provide a wide range of bandgap engineering spanning from 2.4 to 7.8 eV that is highly favorable for device applications. The (Cd, Mg, Zn)O alloy system, however, has both wurtzite (ZnO) and rocksalt (CdO, MgO) crystalline phases. The strong polarization associated with the wurtzite phases of these alloys makes it desirable to achieve growth along nonpolar crystalline directions, such that the polar *c*-axis is in plane. Advantages of nonpolar growth include improved optical efficiency for quantum wells[1,2] and in-plane piezoelectric effects. Nonpolar epitaxial growth of ZnO has been previously studied to achieve *a*-plane ZnO on *r*-plane sapphire[3–6] and *m*-plane ZnO on *m*-plane sapphire.[6] Alternatively, cubic substrates may be utilized to achieve nonpolar ZnO growth.

The integration of ZnO with cubic crystalline materials is of interest due to the potential for heterojunctions consisting of both wurtzite and rocksalt phases of the (Cd, Mg, Zn)O alloy, or other ZnO/cubic heterostructures. A significant advantage and unparalleled property of ZnO in comparison to other compound semiconductors is its chemical compatibility with other oxide materials. This is particularly important in the case of integrating ZnO with materials providing unique functional properties such as ferroelectricity and ferromagnetism. These properties are widely found in cubic perovskite oxides. The ability to interchangeably combine wurtzite and cubic forms of (Cd, Mg, Zn)O alloys, as well as cubic oxides such as perovskites, would therefore provide a powerful method of electronic, optoelectronic, and new multifunctional devices. In this work, the epitaxial growth of ZnO on cubic MgO is described to explore this possibility. The epitaxial growth of wurtzite structures on cubic substrates typically utilizes the (111) orientation due to the hexagonal symmetry,[7,8] resulting in polar growth with *c*-plane orientation. In this work we study the growth of wurtzite ZnO on (001) MgO with the goal of achieving nonpolar ZnO growth while also integrating the wurtzite/cubic structures.

ZnO thin films were grown on MgO (001) substrates by molecular beam epitaxy (MBE) using a two-zone zinc effusion cell and electron cyclotron resonance oxygen plasma source. Prior to ZnO growth, MgO substrates were thermally cleaned at 400 °C and subjected to oxygen plasma for 60 min. A clear MgO (2×1) pattern was observed by reflection high energy electron diffraction (RHEED) through this plasma cleaning procedure. ZnO was then grown at a substrate temperature of 350 °C with a beam equivalent pressure of 1×10^{-6} Torr for the zinc source. An oxygen flow rate of 2.5 SCCM (SCCM denotes cubic centimeter per minute at STP) was used, resulting in an oxygen partial pressure of 5×10^{-5} Torr.

Upon nucleation, the RHEED pattern transitioned to a spotty (4×4) pattern, rather than the (3×3) pattern typically observed for *c*-plane ZnO growth. Four samples were grown in total with a growth rate of 0.1 μm/h and total sample thicknesses ranging between 60 and 120 nm. Initial comparisons were made to ZnO thin films grown by pulsed laser deposition (PLD) on MgO (001) substrates. ZnO thin films were grown by PLD using a KrF excimer laser ($\lambda=248$ nm) with 6 Hz repetition rate and fluence of 1.6 J/cm^2, oxygen partial pressure of 10 mTorr, and substrate temperature of 600 °C. Structural characteristics of the thin films were determined by x-ray diffraction and transmission electron microscopy (TEM). X-ray diffraction measurements consisted of θ-2θ scans and pole figures using a Rigaku rotating anode x-ray generator and diffractometer. Cross-sectional TEM was performed using a Jeol JEM 3010 microscope operated at 300 kV.

The crystalline orientations as determined by x-ray diffraction θ-2θ scans are shown in Fig. 1 for ZnO deposition by both MBE and PLD. This scan was performed on 90 nm thick ZnO films. A preferential orientation of ZnO in the $(10\bar{1}0)$ orientation is inferred for the MBE sample based on the strong peak at 31.8°. A weak peak corresponding to the

a)Electronic mail: cagin@eecs.umich.edu.

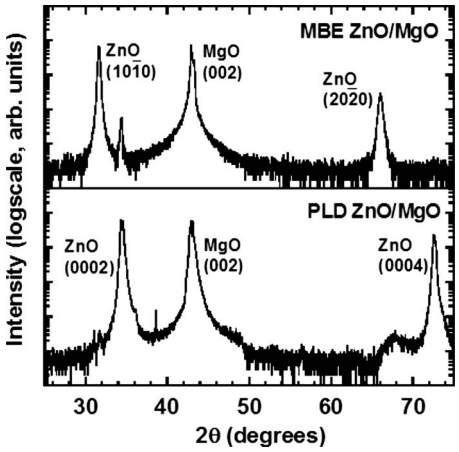

FIG. 1. X-ray diffraction θ-2θ scans of ZnO thin films on MgO substrates.

commonly observed (0002) ZnO diffraction peak is present at 34.4°. In contrast, the PLD sample shows a preferred *c*-plane orientation based on the strong (0002) ZnO peak. It should be noted that epitaxial growth for both *c*-plane ZnO on *c*-plane sapphire and *a*-plane ZnO on *r*-plane sapphire is routinely achieved using the same PLD process. This result stresses the sensitivity of achieving the *m*-plane ZnO orientation for growth on MgO (001), where growth techniques with excellent control over nucleation conditions (such as MBE) are critical in achieving this behavior. All four samples grown by MBE demonstrate similar characteristics with a dominant peak corresponding to *m*-plane orientation, and a weak peak corresponding to *c*-plane growth. The origin of the weak *c*-plane reflection for the MBE samples is believed to be select nucleation sites at particulates or other substrate defects, where polycrystalline growth with preferential *c*-axis growth would dominate. In the remainder of this article, discussion will be limited to the ZnO samples grown by MBE.

A cross-sectional TEM micrograph is shown in Fig. 2, indicating an abrupt ZnO/MgO interface. Independent secondary ion mass spectroscopy measurement conducted on one of the samples further demonstrates an abrupt transition between Mg and Zn elements near the interface. A high resolution TEM micrograph near the interface is shown in Fig. 2. The insets in Fig. 2(b) show digital diffraction patterns (DDPs), which indicate interplanar spacing and phase for the ZnO and MgO, respectively. The DDPs are obtained by fast Fourier transform of the marked square regions in the TEM image. A selected area diffraction pattern (SADP) including both the ZnO thin film and MgO substrate is obtained during the TEM observation, as shown in Fig. 3. Strong diffraction spots are observed for (10$\bar{1}$0) ZnO and (00$\bar{2}$) MgO with a clear indication of the *m*-plane ZnO orientation on MgO (001), as suggested by x-ray diffraction. The interplanar spacing for the (10$\bar{1}$0) plane is calculated using this SADP, and a value of $d=2.82$ Å is obtained. This value agrees closely with the interplanar spacing of $d=2.81$ Å for the x-ray diffraction peak at $2\theta=31.9°$. The lattice constant for an interplanar spacing of $d=2.82$ Å and (10$\bar{1}$0) orientation results in a value of $a=3.25$ Å, which is in close agreement to the lattice constant of $a=3.26$ Å for bulk ZnO.

The SADP of the ZnO/MgO interface also shows a weak ring pattern, indicating some degree of polycrystalline growth. The SADP does not offer a clear indication of the

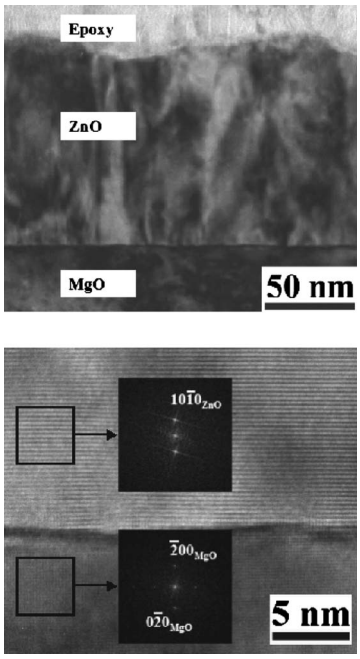

FIG. 2. TEM micrographs of (a) bright field image for the full ZnO/MgO epitaxial layer and (b) high resolution image for the ZnO/MgO interface region. The insets show DDPs obtained from the marked square regions.

in-plane lattice relationships. Alternatively, x-ray diffraction pole figures provide further information on the texture of the ZnO thin film. The pole figure for the (11$\bar{2}$0) ZnO diffraction at $2\theta=56.6°$ is shown in Fig. 4. Reflections are observed near $\chi=30°$, as predicted for the *m*-plane (10$\bar{1}$0) ZnO orientation. This further confirms the *m*-plane relationship, where the more commonly observed *c*-plane (0001) ZnO orientation would not show such reflections due to the orthogonal (11$\bar{2}$0) and (0001) ZnO planes. Eight distinct reflections are observed in the pole figure, in contrast to the expectation of two reflections for single-crystal ZnO. We believe that the eight reflections correspond to two families of domains at 90° for [110] and [1$\bar{1}$0] MgO directions, each with an apparent 30° twist. The 30° twist domains are a likely result of large differences in the lattice mismatch along the *c*- and *a*-axis of the ZnO structure, where $a=3.25$ Å and $c=5.21$ Å. X-ray and electron diffraction analyses suggest a nominal epitaxial relationship with (10$\bar{1}$0) ZnO$\|$(001) MgO, [0001] ZnO$\|$[110] MgO, and [0001] ZnO$\|$[1$\bar{1}$0] MgO, each with twist angles of 30°. The resulting lattice mismatch for

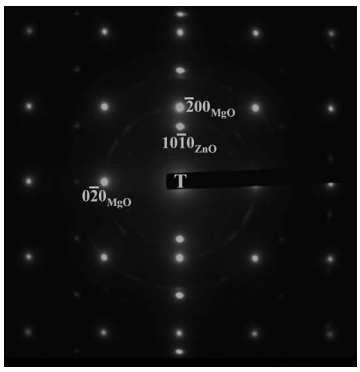

FIG. 3. SADP at the ZnO/MgO interface indicating the *m*-plane ZnO orientation and some degree of polycrystalline feature.

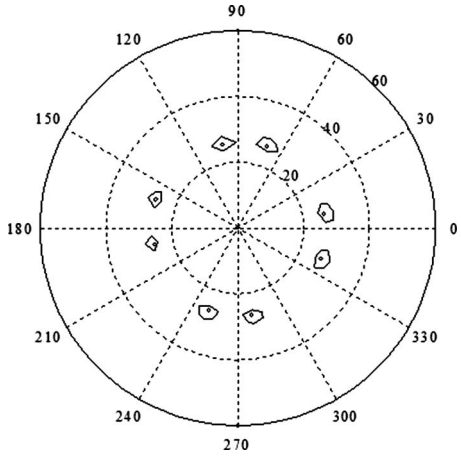

FIG. 4. X-ray diffraction pole figure of the $(11\bar{2}0)$ ZnO reflection at $2\theta = 56.6^{\circ}$ for the *m*-plane ZnO epilayer on MgO. The tilt angle χ and rotation angle φ are defined along the radius and angle of the pole figure, respectively.

this relationship is approximately −9.7% and 12.2% for the *a*- and *c*-directions of ZnO, respectively.

In conclusion, the epitaxial growth of nonpolar *m*-plane ZnO is demonstrated on rocksalt MgO (001) using the MBE growth technique. In contrast, similar experiments using physical vapor deposition techniques such as PLD result in the preferential growth of polar *c*-plane ZnO on MgO (001). TEM observations reveal the abrupt ZnO/MgO interface and confirm the epitaxial *m*-plane ZnO relationship. X-ray diffraction pole figures indicate two preferred rotational domains in-plane with a twist angle of 30°. This work lays foundation for integrating ZnO with a variety of cubic substrates including other II-VI oxides and perovskite oxides, thus leading to novel devices for electronics and optoelectronics applications.

This work was supported by AFOSR under Contract No. FA9550-04-1-0390 and the Center for Optoelectronic Nanostructured Semiconductor Technologies, a DARPA UPR Award No. HR0011-04-1-0040.

[1]J.-M. Chauveau, D. A. Buella, M. Laugt, P. Vennegues, M. Teisseire-Doninelli, S. Berard-Bergery, C. Deparis, B. Lo, B. Vinter, and C. Morhain, J. Cryst. Growth **301-302**, 366 (2007).
[2]C. Chen, V. Adivarahan, J. Yang, M. Shatalov, E. Kuokstis, and M. A. Khan, Jpn. J. Appl. Phys., Part 1 **42**, 1039 (2003).
[3]J. Q. Xie, J. W. Dong, A. Osinsky, P. P. Chow, Y. W. Heo, S. J. Pearton, X. Y. Dong, C. Adelmann, and C. J. Palmstrom, *Progress in Semiconductor Materials V-Novel Materials and Electronic and Optoelectronic Applications*, MRS Symposia Proceedings No. 891 (Materials Research Society, Pittsburgh, 2006), p. 407.
[4]N. W. Emanetoglu, J. Zhu, Y. Chen, J. Zhong, Y. Chen, and Y. Lu, Appl. Phys. Lett. **85**, 3702 (2004).
[5]S. K. Han, S. K. Hong, J. W. Lee, J. Y. Lee, J. H. Song, Y. S. Nam, S. K. Chang, T. Minegishi, and T. Yao, J. Cryst. Growth **309**, 121 (2007).
[6]T. Moriyama and S. Fujita, Jpn. J. Appl. Phys., Part 1 **44**, 7919 (2005).
[7]F. Jiang, C. Zheng, L. Wang, W. Fang, Y. Pu, and J. Dai, J. Lumin. **122-123**, 905 (2007).
[8]T. Matsumoto, K. Nishimura, A. Nishii, A. Ota, Y. Nabetani, and T. Kato, Phys. Status Solidi C **3**, 984 (2006).